Version of Record: https://www.sciencedirect.com/science/article/pii/S1096717623000599
Manuscript_2c7b255ba09e0b8c26baefc257b2fda8

RB-TnSeq identifies genetic targets for improved tolerance of *Pseudomonas putida* towards compounds relevant to lignin conversion

Andrew J. Borchert[1, 2], Alissa Bleem[1, 2], and Gregg T. Beckham[1, 2, *]

[1]Renewable Resources and Enabling Sciences Center, National Renewable Energy Laboratory, Golden, CO, USA
[2]Center for Bioenergy Innovation, Oak Ridge National Laboratory, Oak Ridge, TN, USA
*Corresponding author: gregg.beckham@nrel.gov

Keywords: stress tolerance; acid tolerance; *Pseudomonas putida* KT2440; biological funneling; lignin valorization

ABSTRACT

Lignin-derived mixtures intended for bioconversion commonly contain high concentrations of aromatic acids, aliphatic acids, and salts. The inherent toxicity of these chemicals places a significant bottleneck upon the effective use of microbial systems for the valorization of these mixtures. *Pseudomonas putida* KT2440 can tolerate stressful quantities of several lignin-related compounds, making this bacterium a promising host for converting these chemicals to valuable bioproducts. Nonetheless, further increasing *P. putida* tolerance to chemicals in lignin-rich substrates has the potential to improve bioprocess performance. Accordingly, we employed random barcoded transposon insertion sequencing (RB-TnSeq) to reveal genetic determinants in *P. putida* KT2440 that influence stress outcomes during exposure to representative constituents found in lignin-rich process streams. The fitness information obtained from the RB-TnSeq experiments informed engineering of strains via deletion or constitutive expression of several genes. Namely, Δ*gacAS*, Δ*fleQ*, Δ*lapAB*, Δ*ttgR*::P_{tac}:*ttgABC*, P_{tac}:PP_1150:PP_1152, Δ*relA*, and ΔPP_1430 mutants showed growth improvement in the presence of single compounds, and some also exhibited greater tolerance when grown using a complex chemical mixture representative of a lignin-rich chemical stream. Overall, this work demonstrates the successful implementation of a genome-scale screening tool for the identification of genes influencing stress tolerance against notable compounds within lignin-enriched chemical streams, and the genetic targets identified herein offer promising engineering targets for improving feedstock tolerance in lignin valorization strains of *P. putida* KT2440.

INTRODUCTION

Lignin is an abundant and chemically recalcitrant aromatic heteropolymer that constitutes 15-30% of lignocellulosic biomass from terrestrial plants (Chundawat et al., 2011; Ragauskas et al., 2014). Production of valuable chemicals from lignin has garnered interest as a means to improve the economics and sustainability of traditional biorefineries that target production of biofuels and chemicals from biomass polysaccharides (Becker and Wittmann, 2019; Beckham et al., 2016; Ragauskas et al., 2014; Rinaldi et al., 2016; Schutyser et al., 2018; Sun et al., 2018; Weiland et al., 2021; Zakzeski et al., 2010). A common initial step in lignin valorization involves its depolymerization into a heterogenous mixture of low molecular weight compounds. As an example, alkaline pretreatment of lignocellulosic biomass represents one common strategy for extracting a lignin-rich stream from biomass, commonly referred to as alkaline pretreated liquor (APL), that is enriched in monomeric aromatic compounds. When using corn stover or grasses, these compounds include hydroxycinnamic acids, such as 4-coumaric acid and ferulic acid, acetate from hemicellulose deacetylation, and various aliphatic hydroxy acids, such as lactate and glycolate, that stem from xylose degradation (Gille and Pauly, 2012; Karlen et al., 2020; Karp et al., 2014; Karp et al., 2016; Ralph, 2010). Several microorganisms, such as *Acinetobacter baylyi* (Arvay et al., 2021), *Corynebacterium glutamicum* (Becker et al., 2018), *Rhodococcus opacus* (Henson et al., 2018), *Novosphingobium aromaticivorans* (Cecil et al., 2018; Perez et al., 2022), *Sphingobium* sp. SYK-6 (Masai et al., 2012), and *Rhodosporidium toruloides* (Yaegashi et al., 2017), contain metabolic pathways for the catabolism of lignin-related compounds and organic acids, but the inherent toxicity of these compounds places a significant bottleneck upon the effective use of biological systems for their valorization (Becker and Wittmann, 2019; Klinke et al., 2004; Kohlstedt et al., 2022; Ravi et al., 2019).

Pseudomonas putida KT2440, hereafter KT2440, is a common microbial chassis with industrial potential for the conversion of lignin-derived aromatic compounds into valuable commodities, such as *cis*,*cis*-muconate, β-ketoadipate, and itaconate, among others (Almqvist et al., 2021; Elmore et al., 2021; Johnson et al., 2019; Kohlstedt et al., 2018; Vardon et al., 2015). Underscored by its frequent occurrence in natural environments polluted with toxic chemicals (Kim and Lee, 2011; Orji et al., 2021), KT2440 demonstrates a hardy robustness when challenged by endogenous or exogenous chemical stressors (Chavarria et al., 2013; Dos Santos et al., 2004; Incha et al., 2020; Nikel et al., 2021; Ramos et al., 2009). The metabolic versatility and stress tolerance of KT2440 make it a well-suited platform for the bioconversion of heterogeneous, toxic chemical streams into value-added products (Ankenbauer et al., 2020; Beckham et al., 2016; Borchert et al., 2022b). Nonetheless, the inherent toxicity of many lignin-rich chemical stream constituents still hinders the use of KT2440 as a valorization chassis at the industrial scale (Kohlstedt et al., 2022; Mohamed et al., 2020; Salvachúa et al., 2018).

High-throughput, untargeted approaches, such as transcriptomics, have elucidated KT2440 stress response networks against many types of exogenous stresses (Calero et al., 2018; Gülez et al., 2012; Peng et al., 2018; Roca et al., 2008), and targeted genetic engineering has increased the usefulness of KT2440 as a microbial valorization chassis by ameliorating the toxic effects stemming from exposure to various industrially-relevant chemicals (Basler et al., 2018; Jayakody et al., 2018; Martinez-Garcia et al., 2014). Additionally, transposon insertion sequencing (TnSeq) has aided in the characterization of pathways involved in lignin bioconversion (Cain et al.; Cecil et al., 2018; Eng et al., 2021). A variation of this technique, randomly barcoded (RB)-TnSeq, involves growth of a mutant library generated via insertion of uniquely barcoded transposons at different loci under selective conditions (Wetmore et al., 2015). NGS-mediated enumeration of each barcoded region, pre- and post-selection, helps

determine each the fitness of each mutant, informing gene essentiality for the condition tested. Previously, RB-TnSeq has been applied to interrogate catabolism of aromatic acids, alcohols, fatty acids, lysine, and various nitrogen sources in KT2440 (Incha et al., 2020; Schmidt et al., 2021; Thompson et al., 2019; Thompson et al., 2020). In this work, we employed RB-TnSeq to identify genetic engineering strategies for improving the tolerance of KT2440 against several toxic chemicals found in lignin-enriched process streams.

METHODS

Bacterial strains, plasmids, and primers. Strains used in this work are provided in **Table 1** and are all derivatives of KT2440 (ATCC 47054) (Bagdasarian et al., 1981). Gene disruptions and sequence integrations were performed via allelic exchange using the non-replicative pK18sB vector (Jayakody et al., 2018). Briefly, 800 bp recombination sites with homology to the sequences upstream and downstream of the targeted mutation were encoded onto the pK18sB backbone, which enabled allelic exchange-mediated introduction of the desired mutation into the KT2440 chromosome via a selection (*nptII,* kanamycin)/counterselection (*sacB,* sucrose) strategy (Vardon et al., 2015). A full description of strain construction details as well as a list of plasmids and oligonucleotides are provided in **Tables S1 and S2**. Plasmid construction and storage employed chemically competent NEB 5α F'I^{q} *E. coli* (New England Biolabs, USA). Generally, gene deletions used homology arms encoding ~800 bp upstream of the start codon and ~800 bp downstream of the stop codon for each deleted gene. Introduction of the constitutive *tac* promoter (P_{tac}) (de Boer et al., 1983) involved use of homology arms with a shared sequence for ~800 bp upstream of the native ribosome binding sequence (RBS) (approximated as the 35 bp upstream of the start codon) and ~800 bp encoding the native RBS and ~ 765 bp downstream of the native RBS for each targeted gene. The P_{tac} sequence (5'-gagctgttgacaattaatcatcggctcgtataatgtgtggaattgtgagcggataacaatttcacac-3') was encoded between the two homology arms. All plasmids were assembled using the New England Biolabs Hifi Gibson Mix, and were sequence verified by Genewiz®. Gene deletions and P_{tac} integrations were confirmed by PCR. Correct P_{tac} sequence and CDS sequences for the genes they controlled was confirmed by Sanger sequencing (Genewiz®).

Table 1. Bacterial strains used in this study.

Strains	Genotype	Source
KT2440	pWW0^{-} and restriction^{-} derivative of *P. putida* mt-2	(Bagdasarian et al., 1981)
ML-5	Randomly barcoded Tc1::KT2440 library	(Rand et al., 2017)
AJB187	KT2440 Δ*gacA* Δ*gacS*	This Work
AJB205	KT2440 P_{tac}:*mlaFEDCB*	This Work
AJB206	KT2440 Δ*relA*	This Work
AJB207	KT2440 Δ*oprB-II*	This Work
AJB208	KT2440 P_{tac}:PP_1150:1152	This Work
AJB209	KT2440 Δ*ttgR*:P_{tac}:*ttgABC*	This Work
AJB210	KT2440 P_{tac}:*mlaA*	This Work
AJB211	KT2440 Δ*lapAB*	This Work
AJB212	KT2440 Δ*fleQ*	This Work
AJB219	KT2440 Δ*rlmD:relA*	This Work
AJB225	KT2440 ΔPP_1430	This Work

Culture media and chemicals. Modified M9 (6.78 g/L Na_2HPO_4, 3.00 g/L K_2HPO_4, 0.50 g/L NaCl, 1.66 g/L NH_4Cl, 0.24 g/L $MgSO_4$, 0.01 g/L $CaCl_2$, and 0.002 g/L $FeSO_4$) supplemented with the indicated carbon source(s) was used as minimal medium. Luria-Bertani (LB) medium (Lennox) was the rich medium used. Solid medium involved addition of 1.50% (wt/vol) agar. 50 μg/mL kanamycin was supplemented into the growth medium, when required. Solid sucrose counterselection medium contained 10 g/L yeast extract, 20 g/L tryptone, 250 g/L sucrose, and 3.67% (wt/vol) agar. Stock solutions of all organic acids used in this work (4-coumarate, ferulate, 4-hydroxybenzoate, vanillate, 4-hydroxybenzaldehyde, vanillin, protocatechuate, acetate, lactate, and glycolate) were prepared as 2X solutions and titrated with 5 M NaOH to pH 7.5-8.0 prior to addition (1:1 vol) to 2X M9 medium, prepared separately. Working lactic acid and acetic acid stocks were prepared from an 85% (w/w) DL-lactic acid stock and a reagent grade (>99%) glacial acetic acid stock, respectively. All chemicals for cell culture were purchased from Sigma Aldrich.

Growth quantification. Growth assessment was performed in biological triplicate using a BioLector® automated growth curve analysis system (m2p-labs GmbH). Isolated colonies from an LB plate were inoculated into 100 mm by 13 mm test tubes containing 2 mL LB medium and allowed to grow at 30 °C shaking with 225 rpm overnight (~16 h). For mock APL experiments, isolated colonies from an LB plate were inoculated into 15 mL test tubes containing 4 mL LB medium and incubated for ~14 h at the same speed and temperature. Overnight cultures were used to inoculate (1:100) 1200 μL of M9 minimal medium with the appropriate carbon source in a 48-well FlowerPlate (Beckman-Coulter). Cultures were incubated at 30 °C with shaking at 1200 rpm and 85% humidity. Growth was assessed as the change in measured in arbitrary units [a.u.] of back-scatted 620 nm light with gain set to 3. All growth results were plotted using GraphPad Prism 8.4.2 to generate curves represented as the composite of the averages and standard error of the means (SEM) from the replicates. Biomass measurements (Gain = 3) [a.u.] for all growth data presented in this work were compiled into **Supplementary File 1**.

Transposon library experiments. Experiments employed a KT2440 library (ML-5) harboring randomly-barcoded *mariner* (Tc1) transposon insertions, as described previously (Rand et al., 2017). Three independent 1 mL aliquots of ML-5, which were prepared in LB medium supplemented with kanamycin and stored in 20% glycerol at -80 °C, were thawed on ice and used to inoculate 25 mL of M9 + 20 mM glucose medium in 125 mL baffled flasks. Cultures were grown at 30 °C, shaking at 225 rpm, until reaching an OD_{600nm} of 1.0. A 1 mL aliquot of each library was taken, pelleted (10,000x*g*, 1 min), and stored at -80 °C to later serve as the t_0 of mutant strain abundance. Libraries were then used to inoculate 125 mL baffled flasks containing 25 mL M9 minimal medium with 20 mM glucose and supplemented with either nothing, 60 mM 4-coumarate, 60 mM ferulate, 60 mM 4-hydroxybenzoate, 60 mM vanillate, 10 mM 4-hydroxybenzaldehyde, 10 mM vanillin, 30 mM protocatechuate, 75 mM acetate, 500 mM lactate, 125 mM glycolate, 500 mM NaCl, or 500 mM Na_2SO_4. The stress

concentrations used were those able to elicit a metabolic stress, as accessed by an increase in time to reach stationary phase relative to the no stress control, and within the scope of the concentrations found for these chemicals in lignin-derived chemical streams (Gille and Pauly, 2012; Karp et al., 2014; Karp et al., 2016). Cultures were grown at 30 °C, shaking at 225 rpm, until reaching an OD_{600nm} of 1.0, when 1 mL aliquots were taken, pelleted (10,000x*g*, 1 min), and stored at -80 °C until genomic DNA (gDNA) extraction. The protocatechuate enrichment experiment (with corresponding M9 + 20 mM glucose alone enrichment) was performed on a separate day from all other experiments.

BarSeq. Library preparation, sequencing, and analysis was carried out as described previously (Rand et al., 2017; Wetmore et al., 2015). Briefly, gDNA was obtained from the T=0 and enrichment samples using the GeneJET DNA purification kit (ThermoFisher Scientific). Extracted gDNA was quantified using a NanoDrop™ 2000 spectrophotometer (ThermoFisher Scientific) and each BarSeq PCR reaction was carried out using a common reverse primer (BarSeq_P1) and a unique 6 bp i7 index sequence used for Illumina software-mediated demultiplexing of sequence reads (BarSeq_P2). BarSeq primer sequences are tabulated elsewhere (Wetmore et al., 2015), and are also provided in **Table S3**. Each reaction was performed in 15 µL total volume, using Q5® High-Fidelity 2X Master Mix (New England Biolabs), 0.5 µM of each primer, 100 ng template gDNA, and 2% v/v DMSO. Thermal cycles were: (i) 98 °C – 4 min, (ii) 25 cycles of: 98 °C – 30 s; 55 °C – 30 s; 72 °C – 30 s, (iii) 72 °C – 5 min. Amplification of unique barcode region was confirmed by running 4 µL of each reaction on a 1% w/v agarose gel and visualization of a ~180 bp band. The sequencing pool was generated by combining 8 µL of each PCR product in a single tube and treating with DpnI enzyme (New England Biolabs) using 1 unit DpnI/4.5 µL PCR reaction for 30 min at 37 °C. The entire pool was run on a 1% w/v agarose gel, and the band at ~180 bp was excised and purified using the Zymoclean™ Gel DNA Recovery Kit (Zymo Research). The sample was sequenced on an Illumina HiSeq instrument with 2 x 150 bp reads by Genewiz® (Azenta Life Sciences) and samples were demultiplexed according to their BarSeq P2 indices. Sequencing data (fastq files) were deposited at the NCBI Sequence Read Archive (SRA) with accession number SUB11742400.

Gene fitness calculations. BarSeq reads were analyzed using methods originally described by Wetmore, *et al*. (Wetmore et al., 2015) and modified to include experimental and analytical approaches for improved fitness resolution (Borchert et al., 2022a). Briefly, reads were tabulated according to the number of times each barcode was seen in each sample and the table of barcode counts was then processed according to a table of previously defined genomic barcode locations in the KT2440 library to generate a table (all.poolcount) of tabulated strain counts for each transposon insertion across all samples (**Supplementary File 1**). Transposon insertion counts were used to determine strain fitness calculated as a normalized $\log_2$ ratio of barcode reads in the enrichment sample vs. the baseline sample. Transposon insertion counts were not trimmed from gene ends for fitness calculations. Gene fitness was calculated as the weighted average of the strain fitness for all transposon insertions at that locus and normalized by subtracting the median unnormalized fitness within a 251 gene sliding window. This approach normalizes fitness data such that the typical gene has a fitness of zero, which helps to accurately control against variation in gene copy number, as previously described (Wetmore et al., 2015). If a gene did not contain at least three transposon insertions in the enrichment condition or >30 transposon insertions in the baseline condition, it was excluded from analysis. Comparison of mean fitness values between enrichment and medium reference cultures (M9 + 20 mM glucose alone) was performed using a two-sample *t*-test, where the *p* value was corrected for multiple testing via the positive false discovery rate (pFDR) method (Benjamini and Hochberg, 1995; Storey, 2003). pFDR *q* values were then adjusted for monotonicity (Yekutieli and Benjamini, 1999), and both unadjusted and adjusted *q* values are reported. Gene data were excluded if fitness values were not obtained for all three biological replicates from both conditions. Perl and Python scripts used for fitness calculations and to generate heatmaps, Venn diagrams, and 2D fitness score graphs are accessible from https://github.com/beckham-lab/RB-TnSeq.git.

RESULTS AND DISCUSSION

RB-TnSeq identifies genes that influence fitness during challenge with lignin-related stressors. KT2440 genes involved in stress tolerance against common chemicals found in lignin-rich process streams were identified using RB-TnSeq, where a previously characterized transposon library harboring >185,000 unique barcodes across 5,213 non-essential genes (Rand et al., 2017) was grown in M9 minimal media containing 20 mM glucose and a variety of aromatic acids, aliphatic acids, and sodium (**Figure 1).**.

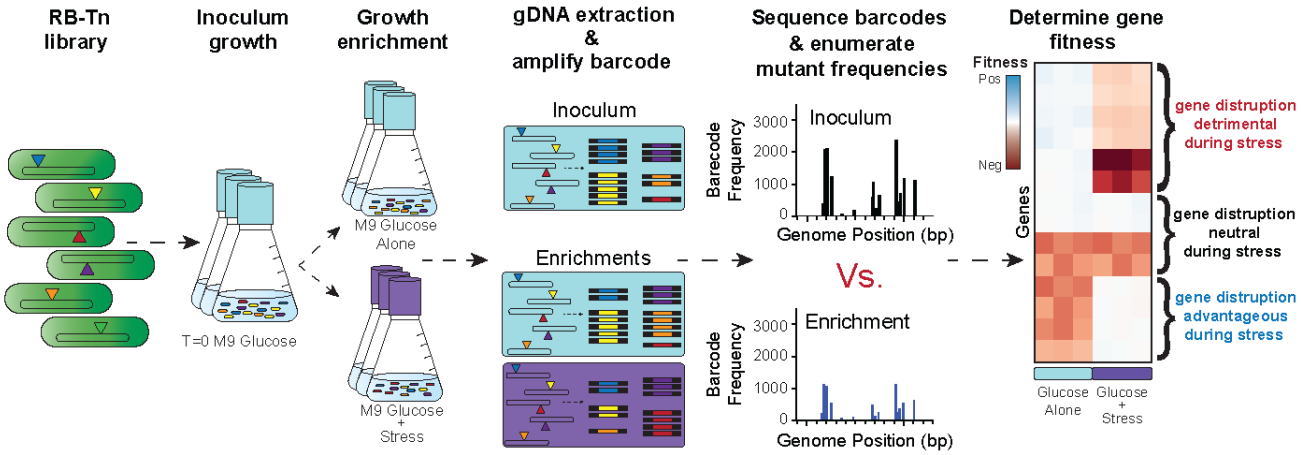

Figure 1. Experimental procedure overview. The ML-5 KT2440 RB-Tn library contains mutants harboring different transposon insertion disruptions throughout the genome, where each disruption encodes a unique barcode sequence. For this study, triplicate cultures of the library was grown in a baseline condition (T=0, M9 + 20 mM glucose) and these cultures were used to inoculate cultures under different selective (enrichment) conditions. Enrichment conditions used were M9 + 20 mM glucose alone (no stress control) and M9 + 20 mM glucose supplemented with stressful quantities of either ferulate, 4-coumarate, vanillin, 4-hydroxybenzaldehyde, vanillate, 4-hydroxybenzoate, protocatechuate, acetate, glycolate, lactate, sodium chloride, or sodium sulfate. The unique barcode sequences were sequenced for both pre- (T=0) and post-enriched cultures, and the frequency of each unique barcode in an enrichment condition vs. its frequency in the baseline condition (T=0) was used to determine gene fitness values for each enrichment condition. Stress-specific fitness effects were then assessed by comparing gene fitness scores obtained following enrichment in the no stress control (glucose only) and enrichments containing glucose with supplemented stressor.

In a method described previously (Wetmore et al., 2015), gene fitness was determined as the relative mutant frequency between populations grown in an enrichment condition and those grown in a baseline ('time zero', T=0) condition used to inoculate the enrichment cultures. Stress conditions consisted of enrichment in M9 minimal medium supplemented with 20 mM glucose and a sublethal concentration of various toxic compounds (**Table S4**). Normalized gene fitness values for the stress enrichments were compared to those for an enrichment performed in M9 + 20 mM glucose alone, to discern stress-specific fitness changes from those general to growth in M9 + glucose (Borchert et al., 2022a). Excluding 4-hydroxybenzoate, all stress enrichment cultures reached an OD_{600nm} = 1.0 later than the M9 + 20 mM glucose control cultures, indicating stress-induced growth inhibition (**Table S4**). Gene fitness scores were calculated for all enrichment conditions, and the results of the fitness comparisons between M9 + glucose vs. M9 + glucose with stressor are provided in **Supplementary File 1**. Positive fitness values indicate that transposon-mediated disruption of a gene led to improved growth of the mutant, while negative fitness values indicate that disruption led to decreased growth of the mutant. Since differences lag times and growth rate can both influence mutant abundance at the time of sampling, it is important to note that what is meant by 'decreased growth' is that the mutant could harbor longer lag times, decreased growth rate, or both.

Disrupting cell-surface adhesion improves fitness across many conditions. Transposon insertion mutants of eight genes were identified that consistently exhibited positive fitness (>0) for most of the 13 enrichment conditions, including for the glucose-only condition (**Figure 2A**). These included transposon mutants of *gacA* (PP_1650) and *gacS* (PP_4099), which encode a two-component signaling system, *fleQ* (PP_4373), which in turn encodes a major flagellar transcriptional regulator, and *lapABCDE* genes, which are involved in cell-surface attachment (El-Kirat-Chatel et al., 2014; Zboralski and Filion, 2020). These findings suggest that disruption of cell-surface adhesion may generally improve growth outcomes in minimal glucose medium, including during metabolic stress.

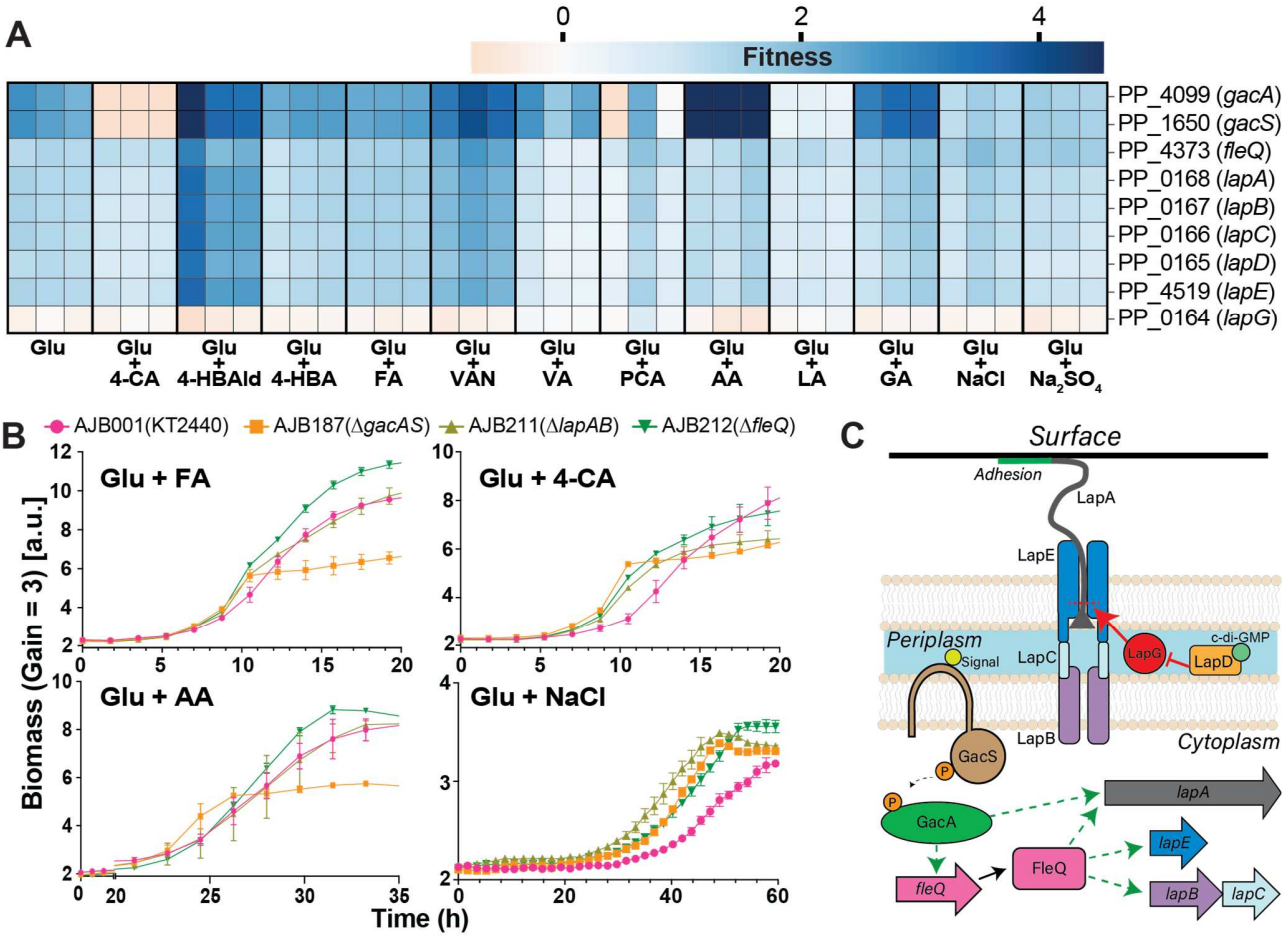

Figure 2. Disruption of the Large adhesion protein (Lap) cell-surface adhesion system generally improves growth outcomes. (**A**) Heatmap of fitness values for 9 genes involved in the Lap system of cell-surface adhesion. 'Glu' refers to the condition in which the library was passaged from T=0 into a second M9 + glucose culture. Generally, disruption of *gacAS*, *fleQ,* or the *lapABCDE* genes led to improved fitness for all the conditions tested in this work. (**B**) Growth of wild-type and mutant strains of KT2440 at 30 °C in M9 medium supplemented with 20 mM glucose and either 100 mM ferulate, 100 mM 4-coumarate, 125 mM acetate, or 1 M NaCl using a BioLector® II. The data represent the mean biomass value, measured in arbitrary units [a.u.] of back-scattered 620 nm light with the gain set to 3, from three biological replicates and error bars denote the standard error of the means. (**C**) Schematic of the *Pseudomonas* Lap system of cell-surface adhesion. LapA is produced in the early stages of biofilm formation and promotes cell-surface attachment. LapBCE form a type I secretion system able to transport LapA to the cell surface. The two-component system, GacAS can activate expression of *lapABCE*, either directly or indirectly through induced expression of *fleQ* (Martínez-Gil et al., 2014; Xiao et al., 2016). The cell adhesion regulator LapG can cleave LapA at the N-terminus in the periplasm, inhibiting surface attachment of planktonic cells or prompting release of attached cells. LapD is activated through binding c-di-GMP, whereupon it sequesters LapG at the inner membrane, promoting the maintenance of intact LapA at the cell surface (Newell et al., 2011; Zboralski and Filion, 2020). Abbreviations are glucose (Glu) 4-coumarate (4-CA), 4-hydroxybenzaldehyde (4-HBAld), 4-hydroxybenzoate (4-HBA), ferulate (FA), vanillin (VAN), vanillate (VA), protocatechuate (PCA), acetate (AA), lactate (LA), and glycolate (GA). Fitness and growth data used for this figure can be found in **Supplementary File 1**.

To test whether elimination of GacAS, FleQ, or the Lap system of cell-surface adhesion would result in improved growth outcomes during growth in media containing several pertinent compounds, Δ*gacAS* (AJB187), Δ*fleQ* (AJB212), and Δ*lapAB* (AJB211) mutants of KT2440 were grown in M9 minimal medium containing glucose and either 100 mM ferulate, 100 mM 4-coumarate, 125 mM acetate, or 1 M NaCl (**Figure 2B**). Relative to wild-type KT2440, the Δ*gacAS*, Δ*lapAB*, and Δ*fleQ* mutants showed moderately decreased lag times during 4-coumarate and sodium chloride stress,. A mild decrease in lag time was also observed during ferulate stress, but this difference was markedly less than observed for 4-coumarate and sodium chloride. Interestingly, the Δ*gacAS* mutant also displayed a lower final biomass yield in the ferulate, 4-coumarate, and acetate conditions (**Figure 2B**), which may indicate that while the Δ*gacAS* mutant improves tolerance against these compounds (assessed by lag times), the resultant regulatory effect from deleting *gacAS* also perturbs carbon assimilation. Conversely, the Δ*gacAS* mutant reached the same final biomass yield as wild-type KT2440 during NaCl stress.

The GacAS two-component system is a global regulator encoded by many *Pseudomonas spp.* and has a pleiotropic role in biofilm formation, antibiotic resistance, iron metabolism, and other secondary metabolism-related pathways (Francis et al., 2017; Huang et al., 2019). Groups have used the regulon characterized in *P. aeruginosa* to predict potential GacAS regulation targets in KT2440 (Eng et al., 2021; Huang et al., 2019; Lim et al., 2022). These bioinformatics data were used to generate a heatmap for fitness associated with disruption of each gene in the potential KT2440 GacAS regulon (**Figure S1**). Interestingly, this analysis revealed that *gacAS* fitness outcomes across all conditions were positively correlated with two other genes that GacAS positively regulates, *fleQ* and *lapA* (Martínez-Gil et al., 2014; Xiao et al., 2016). FleQ plays an important role in the regulation of flagellar biosynthesis and biofilm-formation genes (Molina-Henares et al., 2017), and the *lap* genes are

involved in surface attachment and early biofilm formation, with *lapA* encoding the largest polypeptide in KT2440 (El-Kirat-Chatel et al., 2014; Zboralski and Filion, 2020). A heatmap for fitness associated with disruption of each gene in the KT2440 FleQ regulon, as listed in BioCyc (Karp et al., 2019), also revealed that *fleQ* fitness outcomes across all conditions were most strongly (positively) correlated with those for *lapA lapB*, *lapC*, and *lapD* (**Figure S2**). Since GacAS can activate expression of *lapABCE*, either directly or via induced expression of *fleQ* (Martínez-Gil et al., 2014; Xiao et al., 2016) (**Figure 2C**), these data suggest a model where reduced expression of *lap* genes (mediated through *gacAS* or *fleQ* disruption) or disruption of the *lap* genes themselves results in improved growth in minimal medium, generally.

Importantly, other groups have also identified GacAS, FleQ, and LapAB as potential engineering targets. In KT2440, screening using a muconate-based biosensor revealed that mutants encoding disruptions or deletions of *gacS* demonstrated improved growth and muconate production from glucose (Bentley et al., 2020). Additionally, *gacA* deletion from a KT2440 background improves indigoidine production from 4-coumarate, but not glucose (Eng et al., 2021). Transposon-mediated disruption of *gacS* in *P. putida* CA-3 can also eliminate polyhydroxyalkonoate production (Ryan et al., 2013), and *gacA* or *gacS* deletion in *P. putida* S12 improves tolerance to toluene (Kusumawardhani et al., 2021). In KT2440, strains encoding disruptions of *fleQ* also showed improved growth and muconate production from glucose (Bentley et al., 2020). Additionally, mutations in both *gacS* and *fleQ* were identified in KT2440 mutants adapted against hydroxycinnamic acid stress (Mohamed et al., 2020). Finally, LapA influences the hydrophobicity of cells and has a role in KT2440 tolerance against urea (Reva et al., 2006) and sodium fluoride (Calero et al., 2022). Altogether, disruption of these genes may offer an under-utilized avenue for increasing stress tolerance and production of target bioproducts. However, if the major physiological effect in deleting GacAS and FleQ is via dampening of *lap* gene expression, one strategy may involve deletion of *lap* genes while leaving *gacA*, *gacS*, and *fleQ* intact, to guard against unintended pleiotropic regulatory effects stemming from their deletion.

Disruption of membrane-associated genes reduces fitness during aromatic acid stress. Lignin-rich chemical streams often contain high levels of aromatic acids, such as 4-coumaric acid, ferulic acid, 4-hydroxybenzoic acid, and vanillic acid, and these compounds can exhibit toxicity against KT2440 (Calero et al., 2018; Salvachúa et al., 2018). Transposon mutant enrichment performed in M9 + glucose supplemented with high levels of aromatic acids revealed several genes with significantly (q value < 0.1) altered fitness, compared to the M9 + glucose control condition (**Supplementary File 1**). To determine which genes played roles in tolerance to aromatic acid stress, a set of 58 gene disruptions showing significant fitness effects in two or more of the aromatic acid stress conditions (4-coumarate, 4-hydroxybenzoate, ferulate, vanillate) were identified (**Figure 3 A,B**).

Several of the fitness-disadvantaged genes encoded products commonly associated with the cell membrane (**Figure 3 B,C**). This included genes for the maintenance of lipid asymmetry system (*mlaA* and the *mlaFEDCB* operon), which transports lipids between the inner and outer membrane in Gram-negative bacteria (**Figure 3C**) (Malinverni Juliana and Silhavy Thomas, 2009), the PP_1150-PP_1152 operon, which encodes putative membrane-associated proteins, and the toluene tolerance efflux pump (*ttgABC* operon), which can remove several toxic substances from the cell (**Figure 3C**) (Duque et al., 2001). Consistent with these findings, aromatic compounds, such as 4-ferulate and vanillin, can disrupt membrane integrity, decouple ion gradients, and inhibit cellular respiration in several organisms

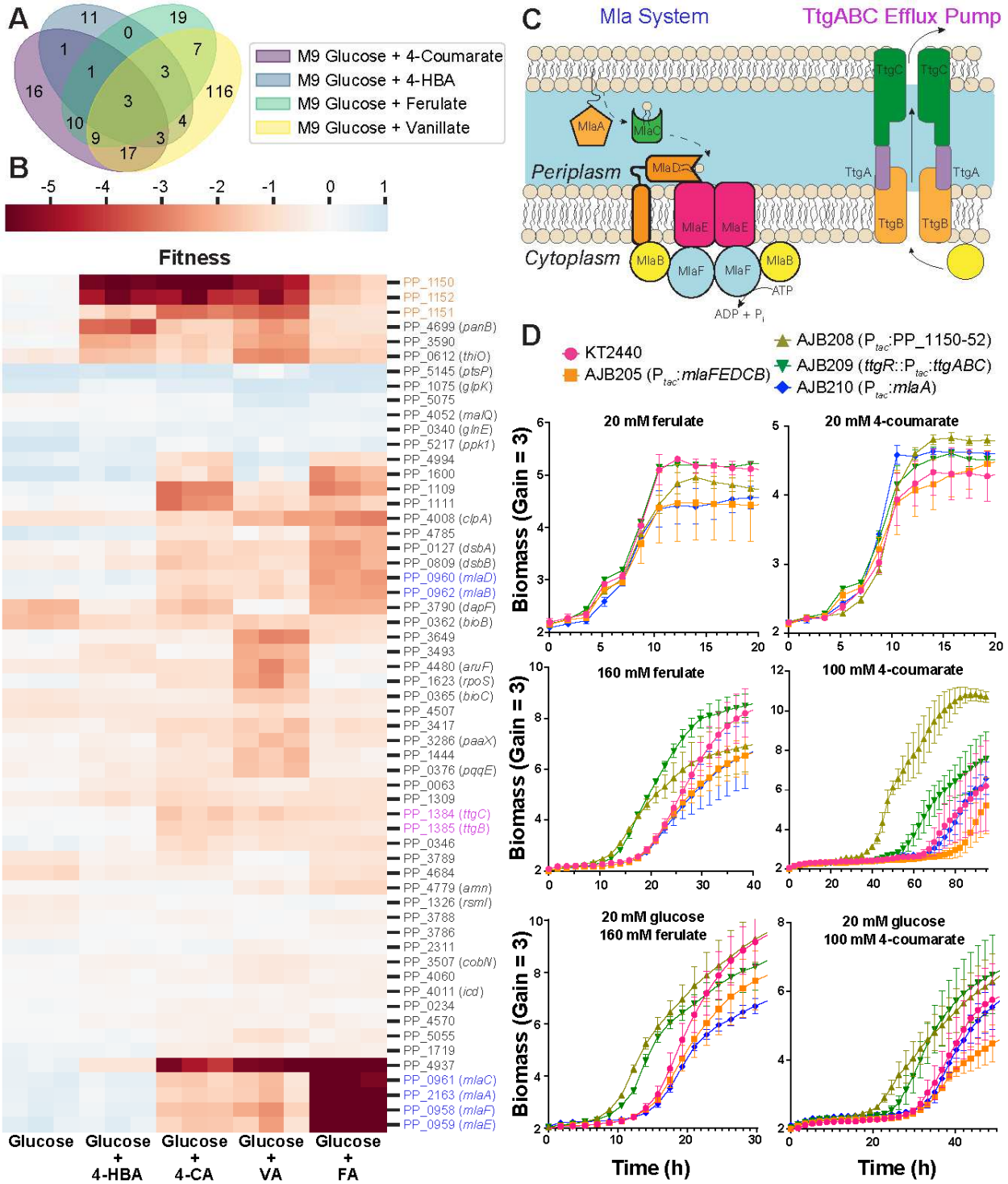

Figure 3. Identification of genes that influence KT2440 aromatic acid tolerance. (**A**) Venn diagram of genes with a significant (q value < 0.1) fitness disparity between M9 + glucose and M9 + glucose with aromatic acid conditions. (**B**) Heatmap of the 58 genes that showed a significant fitness difference for at least two of the aromatic acid stress conditions when compared to the glucose only condition. (**C**) Schematic of the KT2440 Maintenance of lipid asymmetry (Mla) system and the Toluene tolerance genes ABC (TtgABC) efflux pump. The Mla system extracts phospholipids from the outer membrane, traffics them across the periplasmic space, and delivers them to the inner membrane (Malinverni Juliana and Silhavy Thomas, 2009), and TtgABC has broad specificity against several aromatic chemical species (Duque et al., 2001). (**D**) Growth profiles of wild-type and mutant strains of KT2440 during growth at 30 °C in M9 minimal medium supplemented with either 20 mM ferulate, 160 mM ferulate, 20 mM 4-coumarate, 100 mM 4-coumarate, 20 mM glucose and 160 mM ferulate, or 20 mM glucose and 100 mM 4-coumarate. All growth curve values are the mean of three biological replicates and error bars denote standard error of the means. Abbreviations are 4-hydroxybenzoic acid (4-HBA), 4-coumaric acid (4-CA), vanillic acid (VA), ferulic acid (FA), and protocatechuic acid (PCA). Fitness and growth data used for this figure can be found in **Supplementary File 1**.

(Fitzgerald et al., 2004; Luo et al., 2022). Prior work using a different Tn-Seq library also identified several genes encoding membrane-associated proteins as playing a fitness role in tolerance to 4-coumarate in *P. putida* (Calero et al., 2018). Among these genes, in a result consistent with this work, disruption of the *mlaFEDCB* genes showed a strong negative fitness effect during 4-coumarate stress. Additionally, disruption of the *ttgB* gene increases sensitivity to another aromatic compound, toluene (Ramos et al., 1998), and mutants of *P. putida* adapted to growth in ferulate and 4-coumarate contained mutations in *ttgB* (Mohamed et al., 2020). Interestingly, previous work has not identified the PP_1150-52 operon as playing a role in aromatic acid tolerance, though the putative association of these proteins to the membrane and annotation of the PP_1152 gene product as a putative HylD family secretion protein is consistent with this operon encoding another efflux pump. Previous work shows evidence that PP_1150 may be controlled by the histidine kinase, PP_3546 (Sevilla et al., 2013), and is down-regulated when *P. putida* is exposed to high pressures (Follonier et al., 2013); however, the relevance of these findings to hydroxycinnamate stress is unclear.

Interestingly, the set of 58 genes listed in **Figure 3B** did not contain genes commonly associated with the catabolism of 4-hydroxybenzoic acid, 4-coumaric acid, vanillic acid, or ferulic acid (Jimenez et al., 2002), suggesting that catabolism may not play a prominent role during KT2440 stress tolerance against these compounds. This contrasts with the results obtained from enrichment with protocatechuic acid, a shared aromatic acid intermediate formed during the catabolism of 4-hydroxybenzoic acid, 4-coumaric acid, vanillic acid, and ferulic acid, where many of the fitness disadvantaged genes are involved in protocatechuate catabolism, and membrane-associated genes, like the *mla* genes, showed no significant fitness change (**Figure S3, Supplementary File 1**).

To test whether strong constitutive expression of *mlaA*, *mlaFEDCB*, *ttgABC*, or PP_1150-52 would result in improved growth outcomes during 4-coumarate or ferulate stress, P_{tac}:*mlaA* (AJB210), P_{tac}:*mlaFEDCB* (AJB205), P_{tac}:*ttgABC* (AJB209), and P_{tac}:PP_1150-52 (AJB208) mutants of KT2440 were grown in conditions designed to test 4-coumaric acid and ferulic acid stress (**Figure 3D**). The engineered strains were cultivated in minimal medium containing 4-coumaric acid or ferulic acid as the sole carbon and energy sources, using both low stress (20 mM ferulic or 4-coumaric acid) or high stress (160 mM ferulic acid or 100 mM 4-coumaric acid) concentrations of each aromatic acid. The strains were also grown in medium containing 20 mM glucose with either 160 mM 4-coumaric acid or 100 mM ferulic acid. The time taken to reach stationary phase significantly increased for KT2440, when exposed to high 4-coumaric and ferulic acid concentrations, confirming that these concentrations of aromatic acid successfully elicited a metabolic stress (**Figure 3D**).

None of the engineered strains displayed significantly altered growth behavior during growth with 20 mM 4-coumaric or ferulic acid, compared to the KT2440 control (**Figure 3D**). These results indicate that the products of these genes do not significantly alter growth behavior in conditions where relatively low aromatic acid stress is present. However, upon exposure to high levels of 4-coumaric or ferulic acid, both as the sole carbon source and in addition to 20 mM glucose, the P_{tac}:PP_1150-52 and P_{tac}:*ttgABC* mutants showed reduced lag times, compared to the KT2440 parental strain (**Figure 3D**). The P_{tac}:*mlaA* and P_{tac}:*mlaFEDCB* mutants showed no significant change in growth during any stress condition. The failure for constitutive expression of *mlaFEDCB* to improve 4-coumarate or ferulate stress tolerance (**Figure 3D**) may indicate that additional abundance of the Mla complex is inconsequential during stress, but may also indicate that use of the constitutive P_{tac} promoter did not elicit the expected increase in protein abundance, which was not tested in this work.***Disruption of stringent response improves acetate tolerance.*** Lignin-rich chemical streams also often contain high levels of aliphatic acids, such as acetic acid (Karp et al., 2016). High levels of acetate are known to perturb cell growth, which may hamper valorization of streams rich in acetate (Chong et al., 2013; Kirkpatrick et al., 2001). To identify genetic determinants influencing acetate tolerance in KT2440, transposon mutant enrichment was performed in M9 + glucose containing 75 mM acetate. Fitness analysis revealed several genes with significantly (q value < 0.1) altered fitness, as compared to the M9 + glucose control condition (**Figure 4**, **Supplemental File 1**).

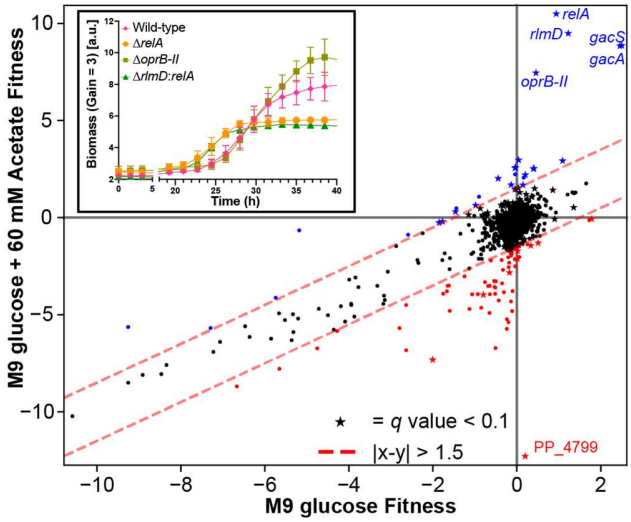

Figure 4. Identification of genes that influence KT2440 tolerance against acetic acid stress. Average normalized gene fitness values for growth in M9 + 20 mM glucose were compared to those for growth in M9 + 20 mM glucose with 75 mM acetic acid. Red dashed lines indicate genes with an average absolute fitness score difference > 1.5. Significance was determined with a two-sample *t*-test, where a q value < 0.1 (stars) denotes a significant fitness disparity between the two conditions. The inset panel is growth of wild-type and mutant strains of KT2440 at 30 °C in M9 medium supplemented with 20 mM glucose and 125 mM acetate using a BioLector® II. The data represent the mean biomass value from three biological replicates and error bars denote the standard error of the means. Fitness and growth data used for this figure can be found in **Supplementary File 1**.

Transposon insertion mutants of five genes were identified that exhibited significantly improved fitness during acetate stress, compared to growth in the M9 + glucose enrichment control (**Figure 4**). In addition to the *gacA/S* genes described in Figure 2, mutants of *oprB*-II (PP_1445), *rlmD* (PP_1655), and *relA* (PP_1656) all had improved fitness. OprB-II forms a small carbohydrate-selective porin that is involved in glucose transport into the periplasmic space (Saravolac et al., 1991; Wylie and Worobec, 1995). Interestingly, adaptive laboratory evolution identified deleterious mutations in *oprB*-II for

KT2440 mutants with improved tolerance against 4-coumarate and ferulate tolerance (Mohamed et al., 2020), but the gene fitness values from RB-TnSeq revealed that an *oprB*-II mutant was severely disadvantaged for growth during vanillate stress (**Supplementary File 1**). RelA is a guanosine tetraphosphate (ppGpp) synthetase, where ppGpp acts as a core signal in the bacterial stringent stress response (Hauryliuk et al., 2015). In KT2440, genes encoding RlmD and RelA are localized adjacent to each other on the chromosome, but do not belong to the same operon. Rather, *rlmD* is annotated as belonging the *cysM-rlmD* operon (Belda et al., 2016). Nonetheless, since several promoters for *relA* are encoded in the coding DNA sequence (CDS) of *rlmD* in *E. coli* (Nakagawa et al., 2006), it is possible that the enrichment of *rlmD* mutants grown under acetate stress was related to a polar effect upon *relA* expression. This idea is bolstered by the observation that mutants harboring transposon insertions in *cysM*, which are expected to disrupt *rlmD* expression without perturbing expression from the *relA* promoters encoded in the *rlmD* CDS, were not enriched during acetate stress (**Supplementary File 1**).

To test whether elimination of RlmD, RelA, or OprB-II led to improved growth outcomes during acetate stress, Δ*oprB-II* (AJB187), Δ*relA* (AJB212), and Δ*rlmD:relA* (AJB211) mutants of KT2440 were grown in M9 + glucose medium with 125 mM acetate (**Figure 4**, inset). The Δ*relA* and Δ*rlmD:relA* mutants both showed reduced lag times but a lower final biomass yield, relative to KT2440 and Δ*oprB-II* strains. This may indicate that these mutations mediated their effect upon lag times through altering assimilation of acetate, glucose, or both. Additionally, if *rlmD* and *relA* disruption independently improved growth outcomes during acetate stress, one would expect the deletion of both genes would lead to better growth outcomes than a mutant where either *rlmD* or *relA* was deleted. Therefore, the observation that Δ*relA* and Δ*rlmD:relA* mutants displayed identical growth behavior further bolstered the hypothesis that disruption of functional RelA expression, and not RlmD itself, was causative of the fitness improvement seen for *rlmD*::Tc1 mutant. These findings help underscore a potential pitfall from TnSeq analysis. Namely, polar effects stemming from insertion of the transposon may lead to the misidentification of genes involved physiological processes. Therefore, it is important to always consider possible polar effects when analyzing TnSeq datasets, particularly for genes contained within operons. Additionally, it is important to consider that gene functional redundancy may also obscure the conclusions made from TnSeq studies.

Relevant to this work, *relA* deletion alters acetate metabolism in *E. coli*, where Δ*relA* mutants accumulate less acetate in the growth medium (Carneiro et al., 2012). It is possible that any shifts in acetate metabolism caused by deletion of *relA*, and the consequence these have upon ppGpp synthesis, allow KT2440 to better adapt to conditions involving acetate stress, reducing the lag time observed prior to growth.

Identification of genes influencing sodium tolerance. Prior to microbial conversion, APL must be neutralized to a pH capable of supporting microbial growth. This is often accomplished through sulfuric acid addition (Rodriguez et al., 2017; Salvachúa et al., 2015) yielding Na_2SO_4. Additionally, many lignin valorization strategies involve the production of dicarboxylic acids, which require neutralization (often using NaOH) to control growth medium pH over the course of the bioconversion process (Salvachúa et al., 2018). Altogether, pH control of the feedstock or growth medium involves the addition of large amounts of salt, which can result in a substantial ionic and osmotic challenge to KT2440, impeding its growth (Costa-Gutierrez et al., 2020).

Transposon mutant enrichment performed in M9 + glucose medium supplemented with high levels of NaCl or Na_2SO_4 revealed several genes with significantly (q value < 0.1) altered fitness, as compared to the M9 + glucose enrichment control (**Supplementary File 1**). To isolate genes with broad roles in sodium tolerance, a set of 33 gene disruptions were identified that showed significant fitness changes during both NaCl and Na_2SO_4 stress (**Figure 5 A,B**). Of these genes, a disruption in PP_1430, which encodes a DegP-like serine endoprotease, appeared to improve fitness during sodium stress. Surprisingly, work in other organisms has revealed that DegP-like endoproteases can be up-regulated in response to salt stress (Song et al., 2020) and knockout of *degP* can negatively impact NaCl tolerance (Leandro et al., 2021).

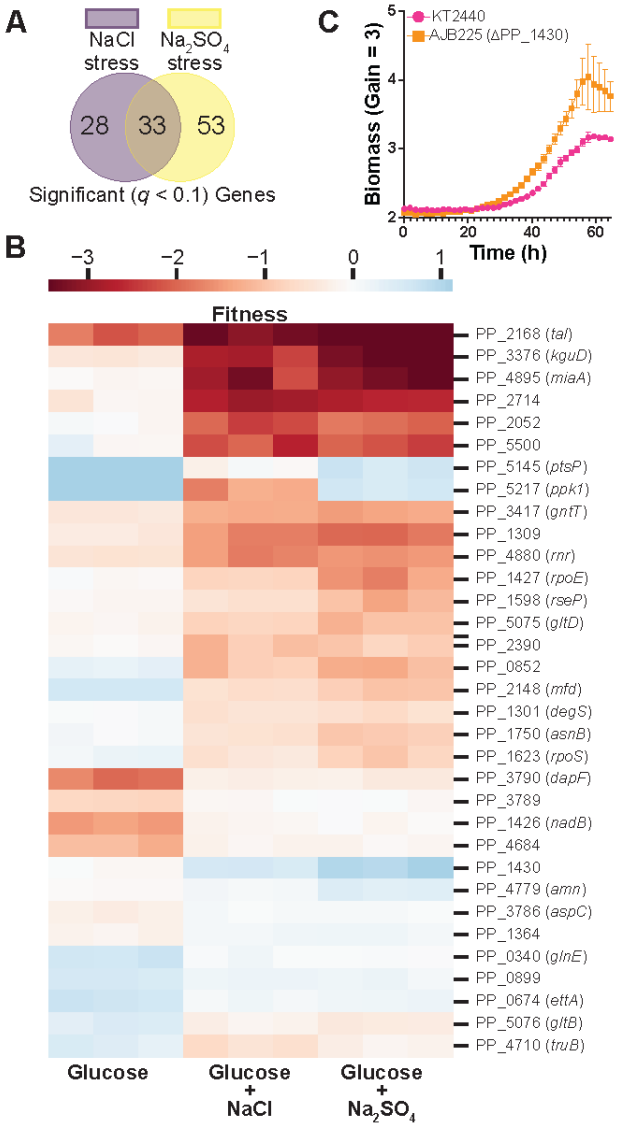

Figure 5. Identification of genes that influence KT2440 sodium (Na^+) tolerance. (**A**) Venn diagram of genes with a significant (q value < 0.1) fitness difference

in. average fitness values between the M9 +20 mM glucose condition and the M9 + 20 mM glucose with 500 mM NaCl or M9 + 20 mM glucose with 500 mM Na_2SO_4 conditions. (**B**) Heatmap of gene fitness values for the 33 genes that showed a significant difference for both NaCl and Na_2SO_4 stress conditions, compared to the glucose only condition. (**C**) Growth profiles of wild-type and a ΔPP_1430 mutant of KT2440 during growth in M9 + 20 mM glucose with 1 M NaCl. Growth curve values are the mean of three biological replicates and error bars denote standard error of the means. Fitness and growth data used for this figure can be found in **Supplementary File 1**.

Nonetheless, in support of the fitness data, a ΔPP_1430 mutant showed decreased lag and a higher final biomass yield, as compared to the parental KT2440 strain, when both were challenged with 1 M NaCl in M9 + glucose medium (**Figure 5C**). Interestingly, disruption of a gene encoding a different KT2440 serine endoprotease, *degS* (PP_1301), led to decreased fitness outcomes during NaCl and Na_2SO_4 stress (**Figure 5B**). Altogether, these data suggest that KT2440 may respond to sodium stress through serine endoprotease-mediated shifts in the proteome.

Many bacteria alter metabolism of amino acids, such as proline, glutamine, and glutamate, when undergoing osmotic stress (Goude et al., 2004; Wood, 2011). This work also revealed that disruption of genes with roles in amino acid metabolism, particularly glutamate and glutamine (e.g. *gltB*, *glnE*, and *gltD*), influenced KT2440 fitness during sodium stress (**Figure 5B**). It is possible that engineered modification of KT2440 glutamate and glutamine metabolism may also be a strategy for improving sodium tolerance in lignin valorization scenarios, which will be investigated in future work.

Assessing mutant growth outcomes on a complex chemical stream. As described above, the RB-TnSeq approach applied in this work identified genetic interventions that improved growth outcomes when KT2440 was subjected to individual stress compounds. However, lignin-enriched biomass hydrolysates are complex heterogenous chemical streams rich in many of these individual stress compounds. To investigate whether the genetic interventions described above would also improve growth of KT2440 in media supplemented with a more complex mixture of chemical stressors, several of the KT2440 mutants described above were grown in M9 minimal medium containing a 'mock APL' mixture as the carbon and energy source. Mock APL was designed to resemble the aromatic and aliphatic acid composition of corn stover APL following treatment with 250 mg NaOH per g dry stover at 130 ºC (Gille and Pauly, 2012; Karp et al., 2014; Karp et al., 2016) and was used in place of a real APL stream to avoid possible confounding results associated with batch-to-batch variability stemming from changes in differences in feedstock composition, treatment conditions, degradation over time, etc. The chemical composition of mock APL was 30 mM 4-coumarate, 20 mM ferulate, 6 mM vanillate, 44 mM acetate, 63 mM lactate, and 60 mM glycolate, neutralized to pH ~7 through titration with NaOH. Notably, mock APL does not contain other trace chemicals found in real APL streams, such as vanillin, but was designed to be generally representative of the high concentration chemical species found in real corn stover APL.

Overall, the Δ*gacAS* and *ttgR*::P_{tac}:*ttgABC* mutant strains showed reduced lag times, relative to the parental KT2440 strain, when grown in the 'mock APL' medium (**Figure 6**). The Δ*fleQ* strain also reached a higher final biomass density than the parental KT2440 strain. This demonstrates that improving KT2440 tolerance against specific chemical stressors may also result in improved growth outcomes in more complex media that contains a mixture of these chemical stressors. Interestingly, the P_{tac}:PP_1150-52 strain showed a significant increase in lag time in mock APL medium, despite its decreased lag relative to the parental KT2440 strain when experiencing ferulate or 4-coumarate stress (**Figure 3D**). This finding underscores how a mutant with improved stress outcomes against a single compound found in lignin-related streams may not retain an advantage against the lignin-related stream itself. Consistent with the data presented in **Figure 3C** and **Figure 4**, the Δ*gacAS*, Δ*relA*, and Δ*rlmD:relA* mutants also displayed a lower final biomass density compared to wild-type KT2440 (**Figure 6**). This may indicate that these mutations perturb assimilation of the carbon present in mock APL.

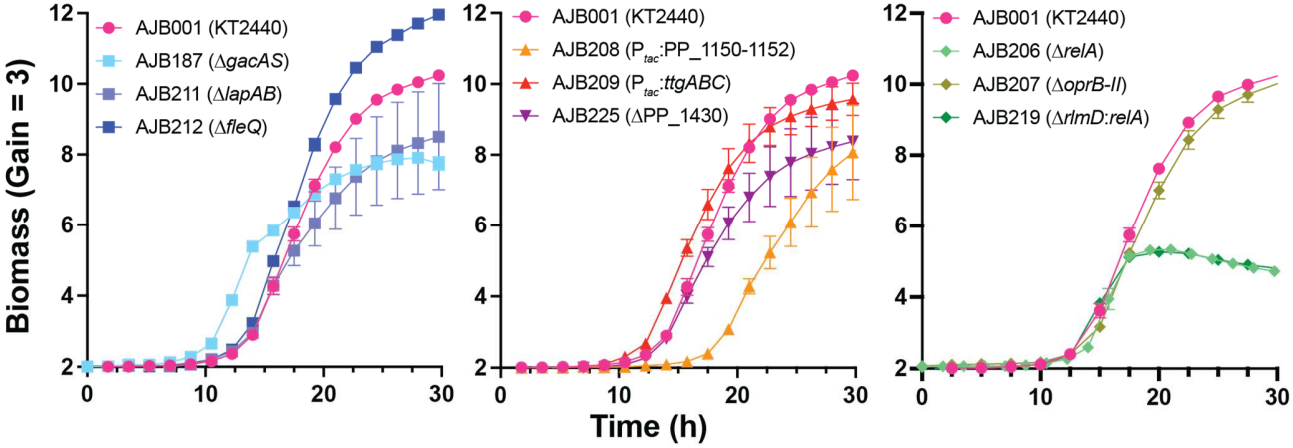

Figure 6. Growth of wild-type and mutant strains of KT2440 at 30 °C in M9 medium supplemented with mock APL (30 mM 4-coumarate, 20 mM ferulate, 6 mM vanillate, 44 mM acetate, 63 mM lactate, and 60 mM glycolate) using a BioLector® II. The data represent the mean biomass value, measured in arbitrary units [a.u.] of back-scatted 620 nm light with gain set to 3, from three biological replicates and error bars denote the standard error of the means from three biological replicates. Growth data used to generate this figure can be found in **Supplementary File 1**

CONCLUSIONS

Generally, this work demonstrates the effectiveness of using RB-TnSeq to identify genetic determinants influencing growth outcomes of a microbe experiencing chemical stress.

Importantly, the specific findings from this work help lay the groundwork for engineering KT2440 for improved tolerance against lignin-related compounds, and some of the mutants studied also exhibited improved growth performance when grown using a complex chemical mixture representative of a lignin-rich chemical stream. However, many of the mutations found to improve growth outcomes when KT2440 was challenged against sub-lethal concentrations of a single metabolic stressor did not translate to improved growth outcomes in the presence of a chemical mixture representative of a lignin-rich chemical stream. This suggests that efforts targeting further improvements of KT2440 tolerance to chemicals within lignin-rich streams might make use of heterogeneous chemical mixtures representative of lignin-rich stream, such as mock APL or directly employ the specific chemical streams being targeted for valorization from the catalytic deconstruction of lignin.

ACKNOWLEDGEMENTS

This work was authored in part by the National Renewable Energy Laboratory, operated by Alliance for Sustainable Energy, LLC, for the U.S. Department of Energy (DOE) under Contract No. DE-AC36-08GO28308. We acknowledge funding from The Center for Bioenergy Innovation, a U.S. Department of Energy Research Center supported by the Office of Biological and Environmental Research in the DOE Office of Science. Funding was also provided to GTB by the U.S. Department of Energy Office of Energy Efficiency and Renewable Energy Bioenergy Technologies Office. The views expressed in the article do not necessarily represent the views of the DOE or the U.S. Government. The U.S. Government retains and the publisher, by accepting the article for publication, acknowledges that the U.S. Government retains a nonexclusive, paid-up, irrevocable, worldwide license to publish or reproduce the published form of this work, or allow others to do so, for U.S. Government purposes. We thank Adam Deutschbauer for donating the KT2440 RB-TnSeq library, Ray Henson for providing pRH090, Caroline Amendola for providing pCA010, Gayle Bentley for providing pGB028, and Allison Werner for providing pAW50 & pAW52.

DECLARATION OF INTERESTS

AJB and GTB have filed a patent application on the genetic targets identified in this work.

REFERENCES

Almqvist, H., Veras, H., Li, K., Garcia Hidalgo, J., Hulteberg, C., Gorwa-Grauslund, M., Skorupa Parachin, N., Carlquist, M., 2021. Muconic acid production using engineered *Pseudomonas putida* KT2440 and a guaiacol-rich fraction derived from Kraft lignin. ACS Sustain. Chem. Eng. 9**,** 8097-8106.

Ankenbauer, A., Schafer, R. A., Viegas, S. C., Pobre, V., Voss, B., Arraiano, C. M., Takors, R., 2020. *Pseudomonas putida* KT2440 is naturally endowed to withstand industrial-scale stress conditions. Microb. Biotechnol. 13**,** 1145-1161.

Arvay, E., Biggs, B. W., Guerrero, L., Jiang, V., Tyo, K., 2021. Engineering *Acinetobacter baylyi* ADP1 for mevalonate production from lignin-derived aromatic compounds. Metab. Eng. Commun. 13**,** e00173.

Bagdasarian, M., Lurz, R., Rückert, B., Franklin, F. C., Bagdasarian, M. M., Frey, J., Timmis, K. N., 1981. Specific-purpose plasmid cloning vectors. II. Broad host range, high copy number, RSF1010-derived vectors, and a host-vector system for gene cloning in *Pseudomonas*. Gene. 16**,** 237-47.

Basler, G., Thompson, M., Tullman-Ercek, D., Keasling, J., 2018. A *Pseudomonas putida* efflux pump acts on short-chain alcohols. Biotechnol. Biofuels. 11**,** 136.

Becker, J., Kuhl, M., Kohlstedt, M., Starck, S., Wittmann, C., 2018. Metabolic engineering of *Corynebacterium glutamicum* for the production of cis, cis-muconic acid from lignin. Microb. Cell Fact. 17**,** 115.

Becker, J., Wittmann, C., 2019. A field of dreams: Lignin valorization into chemicals, materials, fuels, and health-care products. Biotechnol. Adv. 37**,** 107360.

Beckham, G. T., Johnson, C. W., Karp, E. M., Salvachúa, D., Vardon, D. R., 2016. Opportunities and challenges in biological lignin valorization. Curr. Opin. Biotechnol. 42**,** 40-53.

Belda, E., van Heck, R. G., José Lopez-Sanchez, M., Cruveiller, S., Barbe, V., Fraser, C., Klenk, H. P., Petersen, J., Morgat, A., Nikel, P. I., Vallenet, D., Rouy, Z., Sekowska, A., Martins Dos Santos, V. A., de Lorenzo, V., Danchin, A., Médigue, C., 2016. The revisited genome of *Pseudomonas putida* KT2440 enlightens its value as a robust metabolic chassis. Environ. Microbiol. 18**,** 3403-3424.

Benjamini, Y., Hochberg, Y., 1995. Controlling the false discovery rate: A practical and powerful approach to multiple testing. J. R. Stat. Soc. Series B Stat. Methodol. 57**,** 289-300.

Bentley, G. J., Narayanan, N., Jha, R. K., Salvachúa, D., Elmore, J. R., Peabody, G. L., Black, B. A., Ramirez, K., De Capite, A., Michener, W. E., Werner, A. Z., Klingeman, D. M., Schindel, H. S., Nelson, R., Foust, L., Guss, A. M., Dale, T., Johnson, C. W., Beckham, G. T., 2020. Engineering glucose metabolism for enhanced muconic acid production in *Pseudomonas putida* KT2440. Metab. Eng. 59**,** 64-75.

Borchert, A. J., Bleem, A., Beckham, G. T., 2022a. Experimental and analytical approaches for improving the resolution of randomly barcoded transposon insertion sequencing (RB-TnSeq) studies. ACS Synth. Biol.

Borchert, A. J., Henson, W. R., Beckham, G. T., 2022b. Challenges and opportunities in biological funneling of

heterogeneous and toxic substrates beyond lignin. Curr. Opin. Biotechnol. 73**,** 1-13.

Cain, A. K., Barquist, L., Goodman, A. L., Paulsen, I. T., Parkhill, J., van Opijnen, T., 2020. A decade of advances in transposon-insertion sequencing. Nat. Rev. Genet. 21**,** 526-540.

Calero, P., Gurdo, N., Nikel, P. I., 2022. Role of the CrcB transporter of *Pseudomonas putida* in the multi-level stress response elicited by mineral fluoride. Environ. Microbiol.

Calero, P., Jensen, S. I., Bojanovic, K., Lennen, R. M., Koza, A., Nielsen, A. T., 2018. Genome-wide identification of tolerance mechanisms toward *p*-coumaric acid in *Pseudomonas putida*. Biotechnol. Bioeng. 115**,** 762-774.

Carneiro, S., Villas-Bôas, S. G., Ferreira, E. C., Rocha, I., 2012. Influence of the RelA activity on *E. coli* metabolism by metabolite profiling of glucose-limited chemostat cultures. Metabolites. 2**,** 717-32.

Cecil, J. H., Garcia, D. C., Giannone, R. J., Michener, J. K., 2018. Rapid, parallel identification of catabolism pathways of lignin-derived aromatic compounds in *Novosphingobium aromaticivorans*. Appl. Environ. Microbiol. 84.

Chavarria, M., Nikel, P. I., Perez-Pantoja, D., de Lorenzo, V., 2013. The Entner-Doudoroff pathway empowers *Pseudomonas putida* KT2440 with a high tolerance to oxidative stress. Environ. Microbiol. 15**,** 1772-85.

Chong, H., Yeow, J., Wang, I., Song, H., Jiang, R., 2013. Improving acetate tolerance of *Escherichia coli* by rewiring its global regulator cAMP receptor protein (CRP). PLoS One. 8**,** e77422.

Chundawat, S. P. S., Beckham, G. T., Himmel, M. E., Dale, B. E., 2011. Deconstruction of lignocellulosic biomass to fuels and chemicals. Annu. Rev. Chem. Biomol. Eng. 2**,** 121-145.

Costa-Gutierrez, S. B., Lami, M. J., Santo, M. C. C., Zenoff, A. M., Vincent, P. A., Molina-Henares, M. A., Espinosa-Urgel, M., de Cristóbal, R. E., 2020. Plant growth promotion by *Pseudomonas putida* KT2440 under saline stress: role of *eptA*. Appl. Microbiol. Biotechnol. 104**,** 4577-4592.

de Boer, H. A., Comstock, L. J., Vasser, M., 1983. The tac promoter: a functional hybrid derived from the trp and lac promoters. Proc Natl Acad Sci U S A. 80**,** 21-5.

Dos Santos, V. A., Heim, S., Moore, E. R., Stratz, M., Timmis, K. N., 2004. Insights into the genomic basis of niche specificity of *Pseudomonas putida* KT2440. Environ. Microbiol. 6**,** 1264-86.

Duque, E., Segura, A., Mosqueda, G., Ramos, J. L., 2001. Global and cognate regulators control the expression of the organic solvent efflux pumps TtgABC and TtgDEF of *Pseudomonas putida*. Mol. Microbiol. 39**,** 1100-6.

El-Kirat-Chatel, S., Beaussart, A., Boyd, C. D., O'Toole, G. A., Dufrêne, Y. F., 2014. Single-cell and single-molecule analysis deciphers the localization, adhesion, and mechanics of the biofilm adhesin LapA. ACS Chem. Biol. 9**,** 485-94.

Elmore, J. R., Dexter, G. N., Salvachúa, D., Martinez-Baird, J., Hatmaker, E. A., Huenemann, J. D., Klingeman, D. M., Peabody, G. L., Peterson, D. J., Singer, C., Beckham, G. T., Guss, A. M., 2021. Production of itaconic acid from alkali pretreated lignin by dynamic two stage bioconversion. Nat. Commun. 12**,** 2261.

Eng, T., Banerjee, D., Lau, A. K., Bowden, E., Herbert, R. A., Trinh, J., Prahl, J.-P., Deutschbauer, A., Tanjore, D., Mukhopadhyay, A., 2021. Engineering *Pseudomonas putida* for efficient aromatic conversion to bioproduct using high throughput screening in a bioreactor. Metab. Eng. 66**,** 229-238.

Fitzgerald, D. J., Stratford, M., Gasson, M. J., Ueckert, J., Bos, A., Narbad, A., 2004. Mode of antimicrobial action of vanillin against Escherichia coli, Lactobacillus plantarum and Listeria innocua. J. Appl. Microbiol. 97**,** 104-13.

Follonier, S., Escapa, I. F., Fonseca, P. M., Henes, B., Panke, S., Zinn, M., Prieto, M. A., 2013. New insights on the reorganization of gene transcription in Pseudomonas putida KT2440 at elevated pressure. Microb Cell Fact. 12**,** 30.

Francis, V. I., Stevenson, E. C., Porter, S. L., 2017. Two-component systems required for virulence in *Pseudomonas aeruginosa*. FEMS Microbiol Lett. 364**,** fnx104.

Gille, S., Pauly, M., 2012. *O*-acetylation of plant cell wall polysaccharides. Front. Plant Sci. 3.

Goude, R., Renaud, S., Bonnassie, S., Bernard, T., Blanco, C., 2004. Glutamine, glutamate, and alpha-glucosylglycerate are the major osmotic solutes accumulated by *Erwinia chrysanthemi* strain 3937. Appl. Environ. Microbiol. 70**,** 6535-41.

Gülez, G., Dechesne, A., Workman, C. T., Smets, B. F., 2012. Transcriptome dynamics of *Pseudomonas putida* KT2440 under water stress. Appl. Environ. Microbiol. 78**,** 676-683.

Hauryliuk, V., Atkinson, G. C., Murakami, K. S., Tenson, T., Gerdes, K., 2015. Recent functional insights into the role of (p)ppGpp in bacterial physiology. Nat. Rev. Microbiol. 13**,** 298-309.

Henson, W. R., Campbell, T., DeLorenzo, D. M., Gao, Y., Berla, B., Kim, S. J., Foston, M., Moon, T. S., Dantas, G., 2018. Multi-omic elucidation of aromatic catabolism in adaptively evolved *Rhodococcus opacus*. Metab. Eng. 49**,** 69-83.

Huang, H., Shao, X., Xie, Y., Wang, T., Zhang, Y., Wang, X., Deng, X., 2019. An integrated genomic regulatory network of virulence-related transcriptional factors in *Pseudomonas aeruginosa*. Nat. Commun. 10**,** 2931.

Incha, M. R., Thompson, M. G., Blake-Hedges, J. M., Liu, Y., Pearson, A. N., Schmidt, M., Gin, J. W., Petzold, C. J., Deutschbauer, A. M., Keasling, J. D., 2020. Leveraging host metabolism for bisdemethoxycurcumin production in *Pseudomonas putida*. Metab. Eng. Comm. 10**,** e00119.

Jayakody, L. N., Johnson, C. W., Whitham, J. M., Giannone, R. J., Black, B. A., Cleveland, N. S., Klingman, D. M., Michener, W. E., Olstad, J. L., Vardon, D. R., Brown, R. C., Brown, S. D., Hettich, R. L., Guss, A. M., Beckham, G. T., 2018. Thermochemical wastewater valorization via enhanced microbial toxicity tolerance. Energy Environ. Sci. 11**,** 14.

Jimenez, J. I., Minambres, B., Garcia, J. L., Diaz, E., 2002. Genomic analysis of the aromatic catabolic pathways from Pseudomonas putida KT2440. Environ Microbiol. 4**,** 824-41.

Johnson, C. W., Salvachúa, D., Rorrer, N. A., Black, B. A., Vardon, D. R., St. John, P. C., Cleveland, N. S., Dominick, G., Elmore, J. R., Grundl, N., Khanna, P., Martinez, C. R., Michener, W. E., Peterson, D. J., Ramirez, K. J., Singh, P., VanderWall, T. A., Wilson, A. N., Yi, X., Biddy, M. J., Bomble, Y. J., Guss, A. M., Beckham, G. T., 2019. Innovative chemicals and materials from bacterial aromatic catabolic pathways. Joule. 3**,** 1523-1537.

Karlen, S. D., Fasahati, P., Mazaheri, M., Serate, J., Smith, R. A., Sirobhushanam, S., Chen, M., Tymokhin, V. I., Cass, C. L., Liu, S., Padmakshan, D., Xie, D., Zhang, Y., McGee, M. A., Russell, J. D., Coon, J. J., Kaeppler, H. F., Leon, N., Maravelias, C. T., Runge, T. M., Kaeppler, S. M., Sedbrook, J. C., Ralph, J., 2020. Assessing the viability of recovery of hydroxycinnamic acids from lignocellulosic biorefinery alkaline pretreatment waste streams. ChemSusChem.

Karp, E. M., Donohoe, B. S., O'Brien, M. H., Ciesielski, P. N., Mittal, A., Biddy, M. J., Beckham, G. T., 2014. Alkaline pretreatment of corn stover: Bench-scale fractionation and stream characterization. ACS Sustain. Chem. Eng. 2**,** 1481-1491.

Karp, E. M., Nimlos, C. T., Deutch, S., Salvachúa, D., Cywar, R. M., Beckham, G. T., 2016. Quantification of acidic compounds in complex biomass-derived streams. Green Chem. 18**,** 4750-4760.

Karp, P. D., Billington, R., Caspi, R., Fulcher, C. A., Latendresse, M., Kothari, A., Keseler, I. M., Krummenacker, M., Midford, P. E., Ong, Q., Ong, W. K., Paley, S. M., Subhraveti, P., 2019. The BioCyc collection of microbial genomes and metabolic pathways. Brief Bioinform. 20**,** 1085-1093.

Kim, L.-H., Lee, S.-S., 2011. Isolation and characterization of ethylbenzene degrading *Pseudomonas putida* E41. J. Microbiol. 49**,** 575.

Kirkpatrick, C., Maurer, L. M., Oyelakin, N. E., Yoncheva, Y. N., Maurer, R., Slonczewski, J. L., 2001. Acetate and formate stress: Opposite responses in the proteome of *Escherichia coli*. J. Bacteriol. 183**,** 6466-6477.

Klinke, H. B., Thomsen, A. B., Ahring, B. K., 2004. Inhibition of ethanol-producing yeast and bacteria by degradation products produced during pre-treatment of biomass. Appl. Microbiol. Biotechnol. 66**,** 10-26.

Kohlstedt, M., Starck, S., Barton, N., Stolzenberger, J., Selzer, M., Mehlmann, K., Schneider, R., Pleissner, D., Rinkel, J., Dickschat, J. S., Venus, J., B.J.H. van Duuren, J., Wittmann, C., 2018. From lignin to nylon: Cascaded chemical and biochemical conversion using metabolically engineered *Pseudomonas putida*. Metab. Eng. 47**,** 279-293.

Kohlstedt, M., Weimer, A., Weiland, F., Stolzenberger, J., Selzer, M., Sanz, M., Kramps, L., Wittmann, C., 2022. Biobased PET from lignin using an engineered *cis*, *cis*-muconate-producing *Pseudomonas putida* strain with superior robustness, energy and redox properties. Metab. Eng. 72**,** 337-352.

Kusumawardhani, H., Furtwängler, B., Blommestijn, M., Kaltenytė, A., Poel, J. v. d., Kolk, J., Hosseini, R., Winde, J. H. d., Björkroth, J., 2021. Adaptive laboratory evolution restores solvent tolerance in plasmid-cured *Pseudomonas putida* S12: a molecular analysis. Appl. Environ. Microbiol. 87**,** e00041-21.

Leandro, M. R., Vespoli, L. S., Andrade, L. F., Soares, F. S., Boechat, A. L., Pimentel, V. R., Moreira, J. R., Passamani, L. Z., Silveira, V., de Souza Filho, G. A., 2021. DegP protease is essential for tolerance to salt stress in the plant growth-promoting bacterium *Gluconacetobacter diazotrophicus* PAL5. Microbiol. Res. 243**,** 126654.

Lim, H. G., Rychel, K., Sastry, A. V., Bentley, G. J., Mueller, J., Schindel, H. S., Larsen, P. E., Laible, P. D., Guss, A. M., Niu, W., Johnson, C. W., Beckham, G. T., Feist, A. M., Palsson, B. O., 2022. Machine-learning from *Pseudomonas putida* transcriptomes reveals its

transcriptional regulatory network. Metab. Eng. 72, 297-310.

Luo, J., McIntyre, E. A., Bedore, S. R., Santala, V., Neidle, E. L., Santala, S., 2022. Characterization of highly ferulate-tolerant *Acinetobacter baylyi* ADP1 isolates by a rapid reverse engineering method. Appl. Environ. Microbiol. 88, e0178021.

Malinverni Juliana, C., Silhavy Thomas, J., 2009. An ABC transport system that maintains lipid asymmetry in the Gram-negative outer membrane. Proc. Natl. Acad. Sci. U.S.A. 106, 8009-8014.

Martinez-Garcia, E., Nikel, P. I., Aparicio, T., de Lorenzo, V., 2014. *Pseudomonas* 2.0: genetic upgrading of *P. putida* KT2440 as an enhanced host for heterologous gene expression. Microb. Cell Fact. 13, 159.

Martínez-Gil, M., Ramos-González, M. I., Espinosa-Urgel, M., 2014. Roles of cyclic Di-GMP and the Gac system in transcriptional control of the genes coding for the *Pseudomonas putida* adhesins LapA and LapF. J. Bacteriol. 196, 1484-1495.

Masai, E., Kamimura, N., Kasai, D., Oguchi, A., Ankai, A., Fukui, S., Takahashi, M., Yashiro, I., Sasaki, H., Harada, T., Nakamura, S., Katano, Y., Narita-Yamada, S., Nakazawa, H., Hara, H., Katayama, Y., Fukuda, M., Yamazaki, S., Fujita, N., 2012. Complete genome sequence of *Sphingobium sp.* strain SYK-6, a degrader of lignin-derived biaryls and monoaryls. Journal of Bacteriology. 194, 534.

Mohamed, E. T., Werner, A. Z., Salvachúa, D., Singer, C. A., Szostkiewicz, K., Rafael Jiménez-Díaz, M., Eng, T., Radi, M. S., Simmons, B. A., Mukhopadhyay, A., Herrgård, M. J., Singer, S. W., Beckham, G. T., Feist, A. M., 2020. Adaptive laboratory evolution of *Pseudomonas putida* KT2440 improves *p*-coumaric and ferulic acid catabolism and tolerance. Metab. Eng. Comm. 11, e00143-e00143.

Molina-Henares, M. A., Ramos-González, M. I., Daddaoua, A., Fernández-Escamilla, A. M., Espinosa-Urgel, M., 2017. FleQ of *Pseudomonas putida* KT2440 is a multimeric cyclic diguanylate binding protein that differentially regulates expression of biofilm matrix components. Res. Microbiol. 168, 36-45.

Nakagawa, A., Oshima, T., Mori, H., 2006. Identification and characterization of a second, inducible promoter of relA in *Escherichia coli*. Genes Genet. Syst. 81, 299-310.

Newell, P. D., Boyd, C. D., Sondermann, H., O'Toole, G. A., 2011. A c-di-GMP effector system controls cell adhesion by inside-out signaling and surface protein cleavage. PLoS Biol. 9, e1000587.

Nikel, P. I., Fuhrer, T., Chavarría, M., Sánchez-Pascuala, A., Sauer, U., de Lorenzo, V., 2021. Reconfiguration of metabolic fluxes in *Pseudomonas putida* as a response to sub-lethal oxidative stress. ISME J. 15, 1751-1766.

Orji, O. U., Awoke, J. N., Aja, P. M., Aloke, C., Obasi, O. D., Alum, E. U., Udu-Ibiam, O. E., Oka, G. O., 2021. Halotolerant and metalotolerant bacteria strains with heavy metals biorestoration possibilities isolated from Uburu Salt Lake, Southeastern, Nigeria. Heliyon. 7, e07512-e07512.

Peng, J., Miao, L., Chen, X., Liu, P., 2018. Comparative transcriptome analysis of *Pseudomonas putida* KT2440 revealed its response mechanisms to elevated levels of zinc stress. Front. Microbiol. 9.

Perez, J. M., Sener, C., Misra, S., Umana, G. E., Coplien, J., Haak, D., Li, Y., Maravelias, C. T., Karlen, S. D., Ralph, J., 2022. Integrating lignin depolymerization with microbial funneling processes using agronomically relevant feedstocks. Green Chem. 24, 2795-2811.

Ragauskas, A. J., Beckham, G. T., Biddy, M. J., Chandra, R., Chen, F., Davis, M. F., Davison, B. H., Dixon, R. A., Gilna, P., Keller, M., Langan, P., Naskar, A. K., Saddler, J. N., Tschaplinski, T. J., Tuskan, G. A., Wyman, C. E., 2014. Lignin valorization: improving lignin processing in the biorefinery. Science. 344, 1246843.

Ralph, J., 2010. Hydroxycinnamates in lignification. Phytochem. Rev. 9, 65-83.

Ramos, J. L., Duque, E., Godoy, P., Segura, A., 1998. Efflux pumps involved in toluene tolerance in Pseudomonas putida DOT-T1E. J Bacteriol. 180, 3323-9.

Ramos, J. L., Krell, T., Daniels, C., Segura, A., Duque, E., 2009. Responses of *Pseudomonas* to small toxic molecules by a mosaic of domains. Curr. Opin. Microbiol. 12, 215-220.

Rand, J. M., Pisithkul, T., Clark, R. L., Thiede, J. M., Mehrer, C. R., Agnew, D. E., Campbell, C. E., Markley, A. L., Price, M. N., Ray, J., Wetmore, K. M., Suh, Y., Arkin, A. P., Deutschbauer, A. M., Amador-Noguez, D., Pfleger, B. F., 2017. A metabolic pathway for catabolizing levulinic acid in bacteria. Nat. Microbiol. 2, 1624-1634.

Ravi, K., Abdelaziz, O. Y., Nobel, M., Garcia-Hidalgo, J., Gorwa-Grauslund, M. F., Hulteberg, C. P., Liden, G., 2019. Bacterial conversion of depolymerized Kraft lignin. Biotechnol. Biofuels. 12, 56.

Reva, O. N., Weinel, C., Weinel, M., Böhm, K., Stjepandic, D., Hoheisel, J. D., Tümmler, B., 2006. Functional

genomics of stress response in *Pseudomonas putida* KT2440. J. Bacteriol. 188**,** 4079-92.

Rinaldi, R., Jastrzebski, R., Clough, M. T., Ralph, J., Kennema, M., Bruijnincx, P. C., Weckhuysen, B. M., 2016. Paving the way for lignin valorisation: Recent advances in bioengineering, biorefining and catalysis. Angew Chem. Int. Ed. Engl. 55**,** 8164-215.

Roca, A., Rodríguez-Herva, J.-J., Duque, E., Ramos, J. L., 2008. Physiological responses of *Pseudomonas putida* to formaldehyde during detoxification. Microb. Biotechnol. 1**,** 158-169.

Rodriguez, A., Salvachúa, D., Katahira, R., Black, B. A., Cleveland, N. S., Reed, M., Smith, H., Baidoo, E. E. K., Keasling, J. D., Simmons, B. A., Beckham, G. T., Gladden, J. M., 2017. Base-catalyzed depolymerization of solid lignin-rich streams enables microbial conversion. ACS Sustain. Chem. Eng. 5**,** 8171-8180.

Ryan, W. J., O'Leary, N. D., O'Mahony, M., Dobson, A. D. W., 2013. GacS-dependent regulation of polyhydroxyalkanoate synthesis in *Pseudomonas putida* CA-3. Appl. Environ. Microbiol. 79**,** 1795-1802.

Salvachúa, D., Johnson, C. W., Singer, C. A., Rohrer, H., Peterson, D. J., Black, B. A., Knapp, A., Beckham, G. T., 2018. Bioprocess development for muconic acid production from aromatic compounds and lignin. Green Chem. 20**,** 5007-5019.

Salvachúa, D., Karp, E. M., Nimlos, C. T., Vardon, D. R., Beckham, G. T., 2015. Towards lignin consolidated bioprocessing: simultaneous lignin depolymerization and product generation by bacteria. Green Chem. 17**,** 4951-4967.

Saravolac, E. G., Taylor, N. F., Benz, R., Hancock, R. E., 1991. Purification of glucose-inducible outer membrane protein OprB of *Pseudomonas putida* and reconstitution of glucose-specific pores. J. Bacteriol. 173**,** 4970-6.

Schmidt, M., Pearson, A. N., Incha, M. R., Thompson, M. G., Baidoo, E. E. K., Kakumanu, R., Mukhopadhyay, A., Shih, P. M., Deutschbauer, A. M., Blank, L. M., Keasling, J. D., 2021. Nitrogen metabolism in *Pseudomonas putida*: functional analysis using random barcode transposon sequencing. Appl. Environ. Microbiol. 88**,** e02430-21.

Schutyser, W., Renders, T., Van den Bosch, S., Koelewijn, S. F., Beckham, G. T., Sels, B. F., 2018. Chemicals from lignin: an interplay of lignocellulose fractionation, depolymerisation, and upgrading. Chem. Soc. Rev. 47**,** 852-908.

Sevilla, E., Silva-Jiménez, H., Duque, E., Krell, T., Rojo, F., 2013. The Pseudomonas putida HskA hybrid sensor kinase controls the composition of the electron transport chain. Environ Microbiol Rep. 5**,** 291-300.

Song, W. S., Kim, S. M., Jo, S. H., Lee, J. S., Jeon, H. J., Ko, B. J., Choi, K. Y., Yang, Y. H., Kim, Y. G., 2020. Multi-omics characterization of the osmotic stress resistance and protease activities of the halophilic bacterium *Pseudoalteromonas phenolica* in response to salt stress. RSC Adv. 10**,** 23792-23800.

Storey, J., D., 2003. The positive false discovery rate: a Bayesian interpretation and the *q*-value. Ann. Stat. 31**,** 2013-2035.

Sun, Z., Fridrich, B., de Santi, A., Elangovan, S., Barta, K., 2018. Bright side of lignin depolymerization: Toward new platform chemicals. Chem. Rev. 118**,** 614-678.

Thompson, M. G., Blake-Hedges, J. M., Cruz-Morales, P., Barajas, J. F., Curran, S. C., Eiben, C. B., Harris, N. C., Benites, V. T., Gin, J. W., Sharpless, W. A., Twigg, F. F., Skyrud, W., Krishna, R. N., Pereira, J. H., Baidoo, E. E. K., Petzold, C. J., Adams, P. D., Arkin, A. P., Deutschbauer, A. M., Keasling, J. D., 2019. Massively parallel fitness profiling reveals multiple novel enzymes in *Pseudomonas putida* lysine metabolism. mBio. 10.

Thompson, M. G., Incha, M. R., Pearson, A. N., Schmidt, M., Sharpless, W. A., Eiben, C. B., Cruz-Morales, P., Blake-Hedges, J. M., Liu, Y., Adams, C. A., Haushalter, R. W., Krishna, R. N., Lichtner, P., Blank, L. M., Mukhopadhyay, A., Deutschbauer, A. M., Shih, P. M., Keasling, J. D., 2020. Fatty acid and alcohol metabolism in *Pseudomonas putida*: Functional analysis using random barcode transposon sequencing. Appl. Environ. Microbiol. 86**,** e01665-20.

Vardon, D. R., Franden, M. A., Johnson, C. W., Karp, E. M., Guarnieri, M. T., Linger, J. G., Salm, M. J., Strathmann, T. J., Beckham, G. T., 2015. Adipic acid production from lignin. Energy Environ. Sci. 8**,** 617-628.

Weiland, F., Kohlstedt, M., Wittmann, C., 2021. Guiding stars to the field of dreams: Metabolically engineered pathways and microbial platforms for a sustainable lignin-based industry. Metab. Eng.

Wetmore, K. M., Price, M. N., Waters, R. J., Lamson, J. S., He, J., Hoover, C. A., Blow, M. J., Bristow, J., Butland, G., Arkin, A. P., Deutschbauer, A., 2015. Rapid quantification of mutant fitness in diverse bacteria by sequencing randomly bar-coded transposons. mBio. 6**,** e00306-15.

Wood, J. M., 2011. Bacterial osmoregulation: a paradigm for the study of cellular homeostasis. Annu. Rev. Microbiol. 65**,** 215-38.

Wylie, J. L., Worobec, E. A., 1995. The OprB porin plays a central role in carbohydrate uptake in *Pseudomonas aeruginosa*. J. Bacteriol. 177**,** 3021-3026.

Xiao, Y., Nie, H., Liu, H., Luo, X., Chen, W., Huang, Q., 2016. C-di-GMP regulates the expression of *lapA* and *bcs* operons via FleQ in *Pseudomonas putida* KT2440. Environ. Microbiol. Rep. 8**,** 659-666.

Yaegashi, J., Kirby, J., Ito, M., Sun, J., Dutta, T., Mirsiaghi, M., Sundstrom, E. R., Rodriguez, A., Baidoo, E., Tanjore, D., Pray, T., Sale, K., Singh, S., Keasling, J. D., Simmons, B. A., Singer, S. W., Magnuson, J. K., Arkin, A. P., Skerker, J. M., Gladden, J. M., 2017. *Rhodosporidium toruloides*: a new platform organism for conversion of lignocellulose into terpene biofuels and bioproducts. Biotechnol. Biofuels. 10**,** 241.

Yekutieli, D., Benjamini, Y., 1999. Resampling-based false discovery rate controlling multiple test procedures for correlated test statistics. J. Stat. Plan. Inference. 82**,** 171-196.

Zakzeski, J., Bruijnincx, P. C., Jongerius, A. L., Weckhuysen, B. M., 2010. The catalytic valorization of lignin for the production of renewable chemicals. Chem. Rev. 110**,** 3552-99.

Zboralski, A., Filion, M., 2020. Genetic factors involved in rhizosphere colonization by phytobeneficial *Pseudomonas* spp. Comput. Struct. Biotechnol. J. 18**,** 3539-3554.